

Computing interaural differences: Supplementary plots

Supplementary plots for

Computing interaural differences through finite element modeling of idealized human heads

- an article in the Journal of the Acoustical Society of America by Tingli Cai, Brad Rakerd and William M. Hartmann

21 August, 2015

Figure names: All figures compare calculations with interaural measurements on a KEMAR manikin. The prefix “2” indicates the second round of measurements with frequency increments of 50 Hz.

Measurements were made in an anechoic room containing only the manikin and one loudspeaker at ear height. The separation was 3 meters. file names: RD2ITD.DAT and RD2ILD.DAT.

Figures with suffix “ITD” refer to interaural time differences

Figures with suffix “ILD” refer to interaural level differences

The dimensions in the table refer to dimensions of the model in the finite element calculations. No dimensions are given when the neck or torso is not included in the model. Calculations assume incoming spherical wave from a point source at 3 meters. The ear angles are 90 degrees per Burkhard and Sachs.

- Spherical head: 17.5 cm is the diameter of a sphere with the standard radius of 8.75 cm initially used by Hartley and Fry and routinely used in spherical modeling.

- Ellipsoidal head: The dimensions for height (h) width (w) and depth (d) are those given by Burkhard and Sachs in their original KEMAR article. This model is sometimes called the “full ellipsoid” to distinguish it from ellipsoids of revolution.

- ER Tall: Ellipsoid of revolution with only the height from Burkhard and Sachs.
- ER Deep: Ellipsoid of revolution with only the depth from Burkhard and Sachs.
- ER Deeper: Ellipsoid of revolution with exaggerated depth - a parametric variation.
- ER Narrow: Ellipsoid of revolution with only the width from Burkhard and Sachs.
- ER Narrower: Ellipsoid of revolution with exaggerated small width - a parametric variation.
- Neck: Ellipsoid with added neck. All dimensions from Burkhard and Sachs.

- Floor torso: Ellipsoid and neck from Burkhard and Sachs. The torso is represented by a floor, which is a horizontal, nominally infinite, plane that intersects the computational sphere such that it is 57 cm in diameter.

- Shallow box torso: Ellipsoid and neck from Burkhard and Sachs. The torso is represented by a rectangular box having a depth equal to the neck diameter to represent shoulders and a width

equal to the shoulder width given by Burkhard and Sachs. The length extends to the bottom of the computational sphere.

- Box torso: Ellipsoid and neck from Burkhard and Sachs. The torso is represented by a rectangular box having a width equal to the shoulder width and a depth equal to the chest depth as given by Burkhard and Sachs. The length extends to the bottom of the computational sphere.
- Short neck: Same as Box torso except that the neck is shorter - a parametric variation.

Table I (all dimensions in cm)								
Name	h	Head w	d	Neck dia	len	Torso depth	width	code
Spherical head	17.5	17.5	17.5	-	-	-	-	SHM
Ellipsoidal head	22.4	15.5	19.1	-	-	-	-	E
ER Tall	22.4	17.5	17.5	-	-	-	-	TALL
ER Deep	17.5	17.5	19.1	-	-	-	-	DEEP
ER Deeper	17.5	17.5	22.4	-	-	-	-	DPR
ER Narrow	17.5	15.2	17.5	-	-	-	-	THIN
ER Narrower	17.5	5.0	17.5	-	-	-	-	FISH
Added Neck	22.4	15.5	19.1	11.3	18.8	-	-	NECK
Floor torso	22.4	15.5	19.1	11.3	18.8	57	57	ENF
Shallow box torso	22.4	15.5	19.1	11.3	18.8	11.3	44	BX11
Box torso	22.4	15.5	19.1	11.3	18.8	19.1	44	ENB
Short neck	22.4	15.5	19.1	11.3	14	19.1	44	NK14

CONTENTS

For ITD:

Page 6: 2SHMITD - spherical head model. Calculated from the formula in Brungart and Rabinowicz for a source distance of 3 m. The low-frequency limit (Kuhn) and high-frequency limit (Woodworth) appear as filled symbols to left and right. The model underestimates the observed dispersion between 500 and 1500 Hz for 20, 30 and 45 degrees. The model badly overestimates the ITD for azimuths of 45 and 60 degrees.

Page 7: 2EITD - ellipsoidal head: The model captures most of the observed dispersion between 500 and 1500 Hz for 20, 30 and 45 degrees. It largely solves the overestimates made by the spherical head model at 45 and 60 degrees. It does not reproduce small peaks and valleys in the experiment; the model functions are too smooth to agree well with the experiment.

Page 8: 2TALLITD - ellipsoid of revolution: Incorporating only the height from the ellipsoid. This parametric variation shows that most of the dispersion captured by the ellipsoidal head model can be obtained by increasing the height of the head. However, overall, the ITDs are too large because the head volume is now too large.

Page 9: 2DEEPITD - ellipsoid of revolution: Incorporating only the depth of the ellipsoid. This parametric variation leads to only a small change compared to the spherical head model with the largest difference being about 20 μ s. Evidently the improvements made by the ellipsoidal model are not because of the depth of the ellipsoid.

Page 10: 2DPERITD - ellipsoid of revolution (deeper than deep head). In this parametric variation, the head is given the unphysically large depth of 22.4 cm. That particular depth was chosen because it is equal to the height of the TALL head that successfully reproduced most of the the dispersion seen in the ellipsoid calculation. The figure compares the DEEP calculation (19.1 cm) with the DEEPER calculation (22.4 cm). There is very little difference, never more than about 20 μ s. Therefore, even the DEEPER calculation fails to obtain the observed dispersion. Because the TALL head and the DEEPER head have the same dimensions it was a surprise to find that the DEEPER head did not reproduce the observed dispersion in the same way that the TALL head did. Apparently the orientation with respect to the incident sound direction is important.

Page 11: 2THINITD - ellipsoid of revolution incorporating only the narrow width of the ellipsoid. This parametric variation significantly reduces the ITD compared to the spherical head model (shown dashed) or the ellipsoidal head model, especially for larger azimuths. The solid and dashed lines are roughly parallel indicating that the narrow head does not capture the observed dispersion.

Conclusion: The three parametric variations indicate that the success of the ellipsoidal head model vis-a-vis the spherical head model (with respect to ITD) is the result of increased dispersion caused by the increased height of the ellipsoid (TALL) coupled with the decreased ITD overall caused by the narrower width (THIN). The depth is not a factor.

Page 12: 2FISHITD - narrower ellipsoid of revolution with dramatically narrowed width. Checks that further narrowing compared to THIN further decreases ITD.

Page 13: 2ENITD - Ellipsoidal head plus added neck. The height, width, depth of the full ellipsoid are equal to those in EITD. The effect of adding the neck alone without the torso might have been predicted from the TALL head calculation because the neck adds to the overall height of the model. Adding the neck increases the dispersion between 500 and 1500 Hz beyond the dispersion seen with the ellipsoid alone. It leads to too much dispersion to agree with experiment.

Page 14: 2ENFITD - ellipsoid, neck, floor torso. This model adds reflections from a torso (modelled as a floor) to the full ellipsoid plus neck. The reflections cause oscillations in ITD that result in better agreement with experiment than calculated for the ellipsoid (2EITD) shown dashed. Although the neck is the same as for 2ENITD, the oscillations compensate the exaggerated dispersion seen for the neck alone. The largest changes that occur when a neck and floor torso are added to the ellipsoidal head are below 500 Hz. One expects to see large geometrical changes like this to lead to changes at long wavelengths.

Page 15: 2BX11ITD - ellipsoid, neck, box torso (11.3 cm - shallow torso) This model adds reflections from a torso (modelled as a rectangular box) to the full ellipsoid plus neck. The box is shallow, having a depth only equal to the neck diameter. The width of the box corresponds to the KEMAR shoulder width. Reflections from this box cause minor oscillations in the ITD function that compensate the excessive dispersion seen for the neck alone (2ENITD). Because of the compensation the ITD resembles the ITD seen for the ellipsoid by itself (2EITD) (shown dashed). There is almost no difference between the two curves.

Page 16: 2ENBITD - ellipsoid, neck, box torso (19.1 cm - thick torso). This model adds reflections from a torso (modelled as a rectangular box) to the full ellipsoid plus neck. The reflections cause oscillations in ITD that result in better agreement with experiment than calculated for the

ellipsoid with the floor (2ENFITD). The improvement over the floor-torso is particularly striking below 500 Hz (except for an azimuth of 90 degrees). Compared to the ellipsoid (2EITD) (shown dashed) the oscillations further improve the dispersion seen between 500 and 1500 Hz for 20, 30, 45, and 60 degrees azimuth. However, a strange structure suddenly appears near 2000 Hz for 60 degrees. That structure looks like a Kramers-Kronig partner for the equally strange peak that occurs in the ILD at this frequency and azimuth (see page 27).

Page 17: 2NK14ITD - ellipsoid, 14-cm neck, box torso (thick torso). This model is identical to 2ENBITD except that the neck length is reduced from 18.8 cm to 14 cm. This calculation was done to test the conjecture that shortening the neck would merely spread the oscillations to wider frequency spacing. That effect was observed (e.g. 45 and 60 degrees), but in addition the shorter neck increased the amplitude of the oscillations. The 14-cm neck did not improve agreement with experiment. It is clearly too short.

For ILD:

Page 18: 2SHMILD - spherical head model. Calculated from the formula in Brungart and Rabinowicz for a source distance of 3 m. The low-frequency limit for plane wave incidence (Rayleigh) appears as a dashed line. The model underestimates the ILD for most frequencies and azimuths with discrepancies as large as 5 dB (60 degrees). It underestimates the peak to valley differences for azimuths of 10, 20, 30, and 45 degrees.

Page 19: 2EILD - ellipsoidal head: The shape of the model function agrees better with experiment than the spherical head function. The 5-dB discrepancy is eliminated. The ellipsoidal head model incompletely removes the peak to valley differences found in the spherical head model at small azimuths. It does not reproduce small peaks and valleys in the experiment; the model functions are too smooth to agree with the experiment.

Page 20: 2TALLILD - ellipsoid of revolution, incorporating only the height from the ellipsoid. This parametric variation shows that most of the improvement over the spherical head model that was captured by the ellipsoidal head can be obtained by increasing the height of the head. That appears particularly for 60 degrees where the spherical head ILD was in greatest disagreement. At 20, 30 and 45 degrees the TALL ellipsoid led to helpful changes from the spherical head that were in the same direction as the full ellipsoid but somewhat smaller in size.

Page 21: 2DEEPILD - ellipsoid of revolution, incorporating only the depth of the ellipsoid. This parametric variation leads to negligible change compared to the spherical head model. Only in a few small ranges of azimuth and frequency are the changes as large as 1 dB.

Page 22: 2DPERILD - ellipsoid of revolution (deeper than deep head). In this parametric variation, the head is given the unphysically large depth of 22.4 cm. That particular depth was chosen because it is equal to the height of the TALL head. The figure compares the DEEP calculation (19.1 cm) with the DEEPER calculation (22.4 cm). There is very little difference, never more than 1 dB except at 60 degrees from 2000 to 2500 Hz where the change is about 1.5 dB. Therefore, even the DEEPER model fails to obtain the improvements seen with the full ellipsoid.

Page 23: 2THINILD - ellipsoid of revolution incorporating only the narrow width of the ellipsoid. This parametric variation leads to very little difference compared to the spherical head model. Therefore, the narrow width of the ellipsoid cannot be responsible for the improved agreement with

experiment when the sphere is replaced by the full ellipsoid. The sign of the difference between the narrow model ILD 2THINILD and the sphere is unexpected. The narrow model leads to a (slightly) larger ILD than the sphere, even though the narrow model is physically smaller than the sphere. (Observe for azimuths of 20, 30, 45 degrees and frequencies above 1000 Hz.

Page 24: 2FISHILD - narrower ellipsoid of revolution with dramatically narrowed width. Checks that further narrowing leads to further increase in ILD compared to the sphere for frequencies greater than 1000 Hz. Apparently this very thin head casts a very deep shadow on the opposite side as the wavelength shrinks to be less than twice the head size ($2 \times 17.5 = 35$) cm.

Conclusion: The three parametric variations indicate that the success of the ellipsoidal head model vis-a-vis the spherical head model (with respect to ILD) is the result of the increased height of the ellipsoid (TALL). The width and depth are not factors.

Page 25: 2ENILD - Ellipsoidal head with added neck. Adding the neck to the full ellipsoid leads to greater differences between peaks and valleys for the ILD, but except for 10 and 20 degrees of azimuth, this structure appears at the wrong frequencies or is too large to agree with experiment. Adding the neck improves agreement compared to the spherical head only at 10 and 90 degrees, possibly at 20 degrees.

Page 26: 2ENFILD - ellipsoid, neck, floor torso. This model adds reflections from a torso (modelled as a floor) to the full ellipsoid. The reflections cause oscillations in ILD that result in better agreement with experiment than calculated for the ellipsoid (2EILD) and much better than for the neck alone (2ENILD) with small exceptions at 10 and 20 degrees.

Page 27: 2ENBILD - ellipsoid, neck, box torso (19.1 cm - thick torso). This model adds reflections from a torso (modelled as a rectangular box) to the full ellipsoid. The reflections cause oscillations in ILD that result in better agreement with experiment than calculated for the ellipsoid with the floor, (2ENFILD) for 10, 20, 30, 45, and 90 degrees. The floor calculation is included in the plot for comparison. For 60 degrees, the box torso leads to an anomalous peak in ILD near 2000 Hz, which wrecks agreement with experiment and makes the box torso look worse than the floor. We can compute the improvement for the box by limiting the frequency range to 1500 Hz because of the larger size of the model when the box is added.

Page 28: 2BX11ILD - ellipsoid, neck, box torso (11.3 cm - shallow torso) This model adds reflections from a torso (modelled as a rectangular box) to the full ellipsoid. The box is shallow, having a depth only equal to the neck diameter. The width of the box corresponds to the KEMAR shoulder width. Reflections from this box cause only minor oscillations in the ILD function and minimal change from the ellipsoid itself (2EILD).

Page 29: 2NK18ILD - ellipsoid, 18-cm neck, box torso (thick torso). This model is identical to 2ENBILD. The only difference is that the comparison is with the spherical head model instead of with the floor torso model.

Page 30: 2NK14ILD - ellipsoid, 14-cm neck, box torso (thick torso). This model is identical to 2ENBILD or 2NK18ILD except that the neck length is reduced from 18.8 cm to 14 cm. This calculation was done to test the conjecture that shortening the neck would merely spread the oscillations to wider frequency spacing. That effect was observed at 30, 45, 60 and 90 degrees, and it made agreement with experiment worse. The addition the shorter neck sometimes increased the amplitude of the oscillations and sometimes decreased the amplitude.

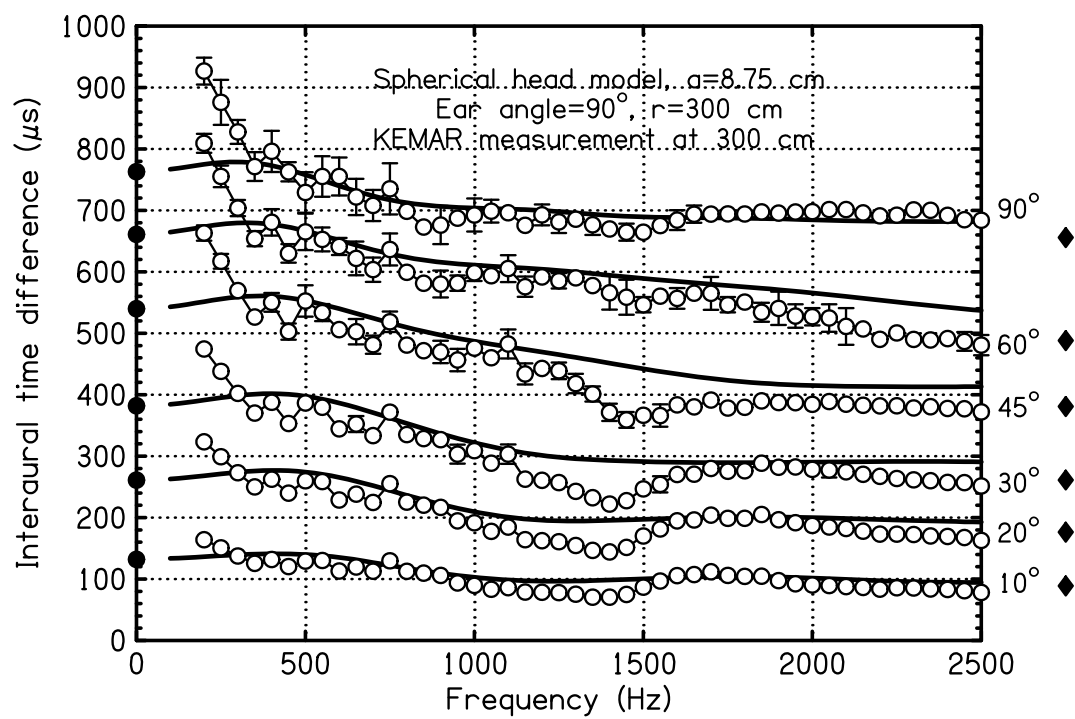


Fig. 2shmitd

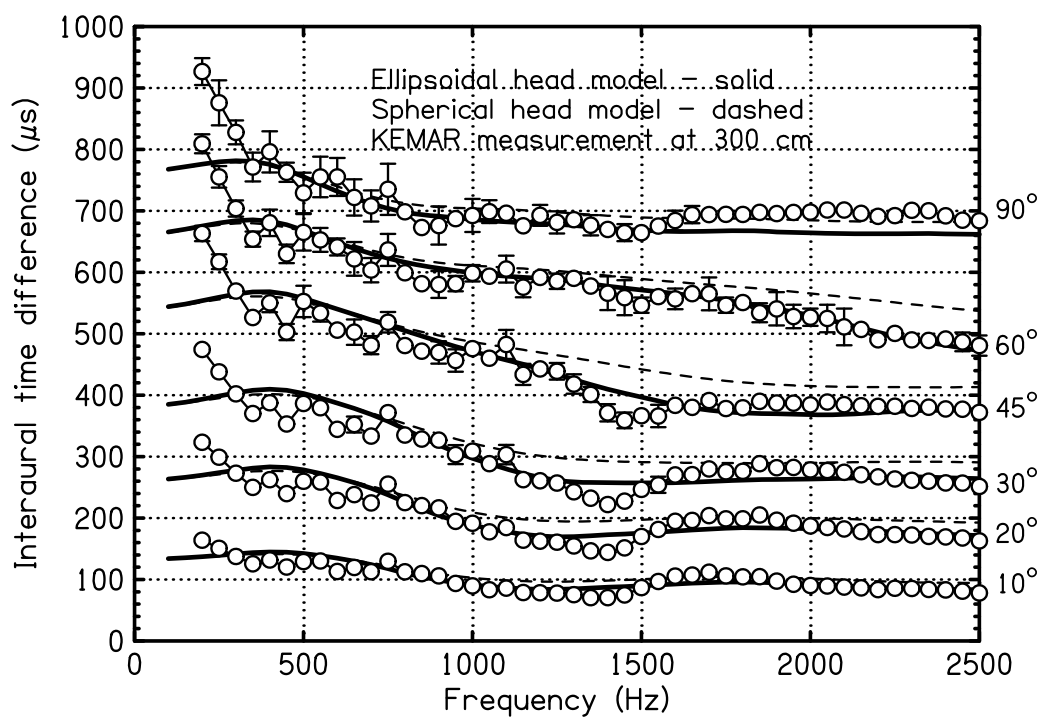


Fig. 2eitd

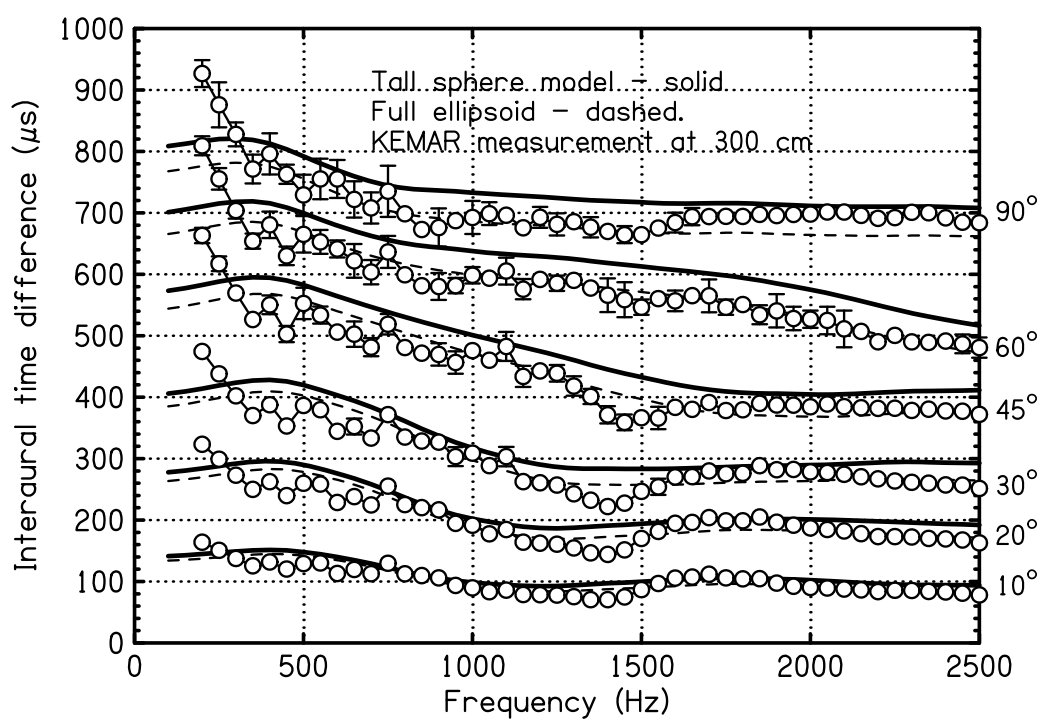


Fig. 2tallitd

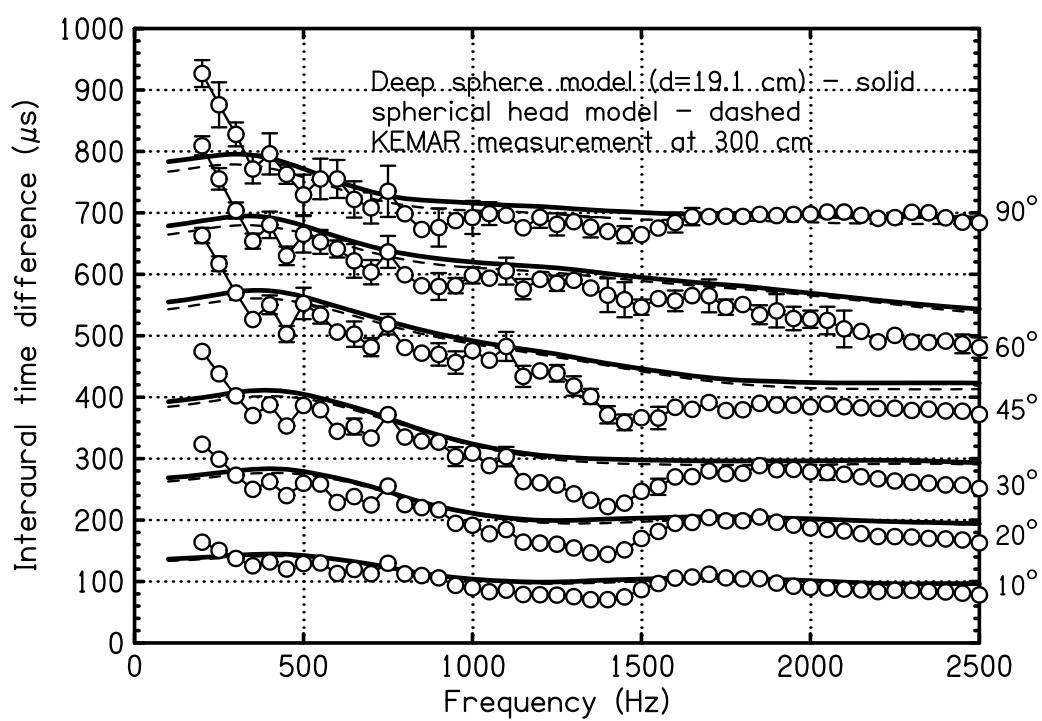


Fig. 2deepitd

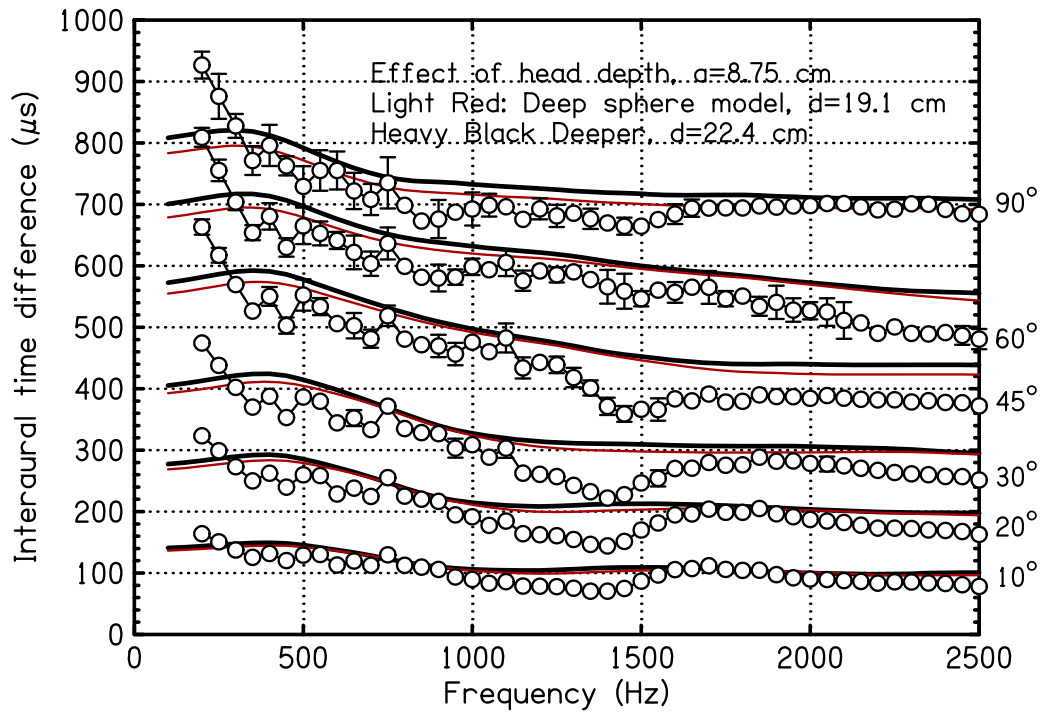


Fig. 2dperitd

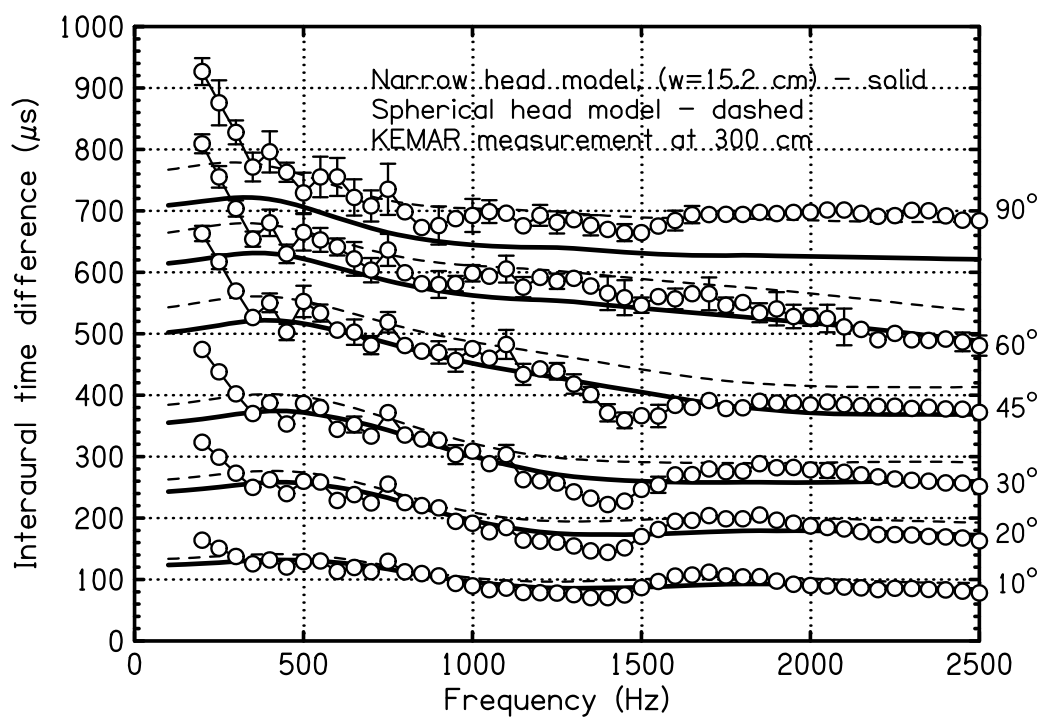


Fig. 2thinitd

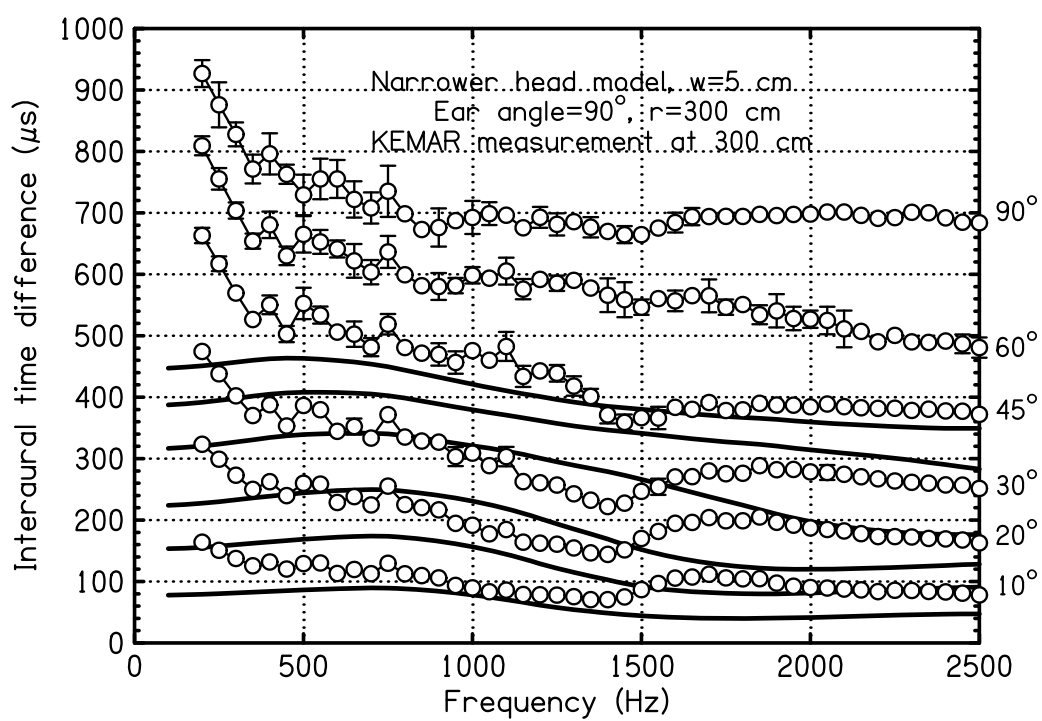


Fig. 2fishitd

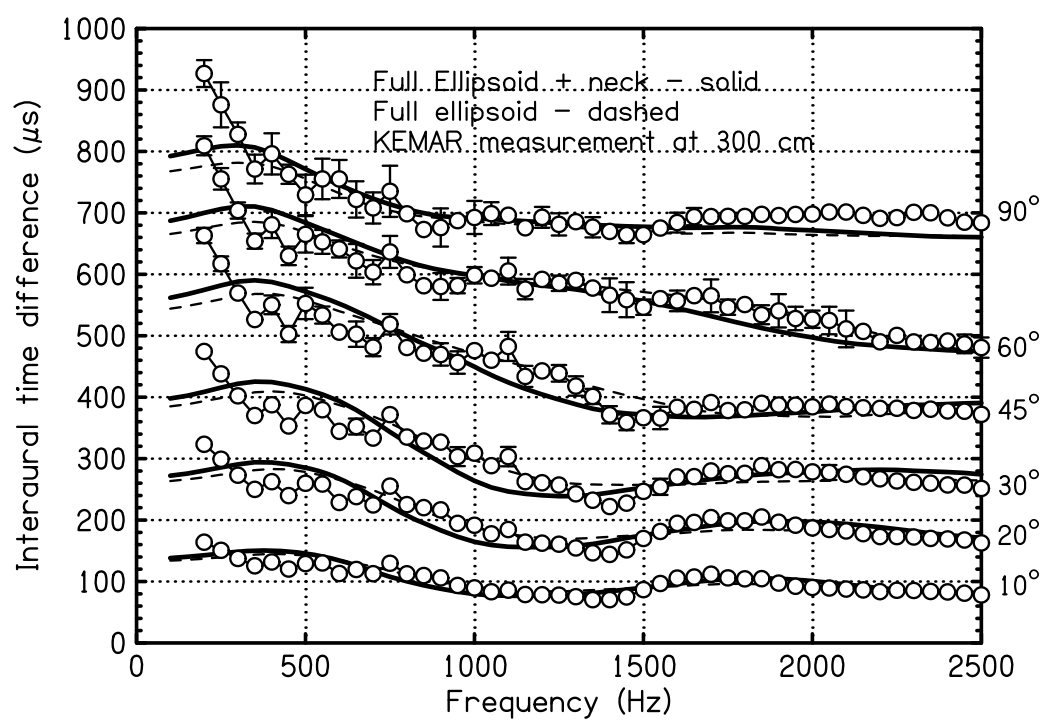


Fig. 2enitd

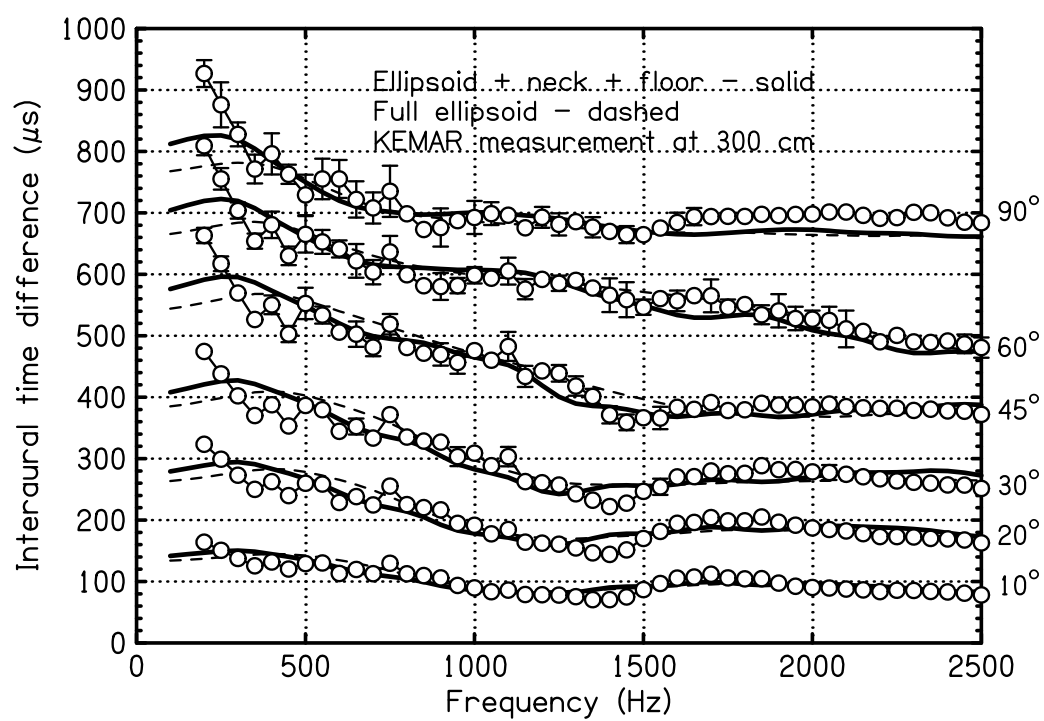


Fig. 2enfitd

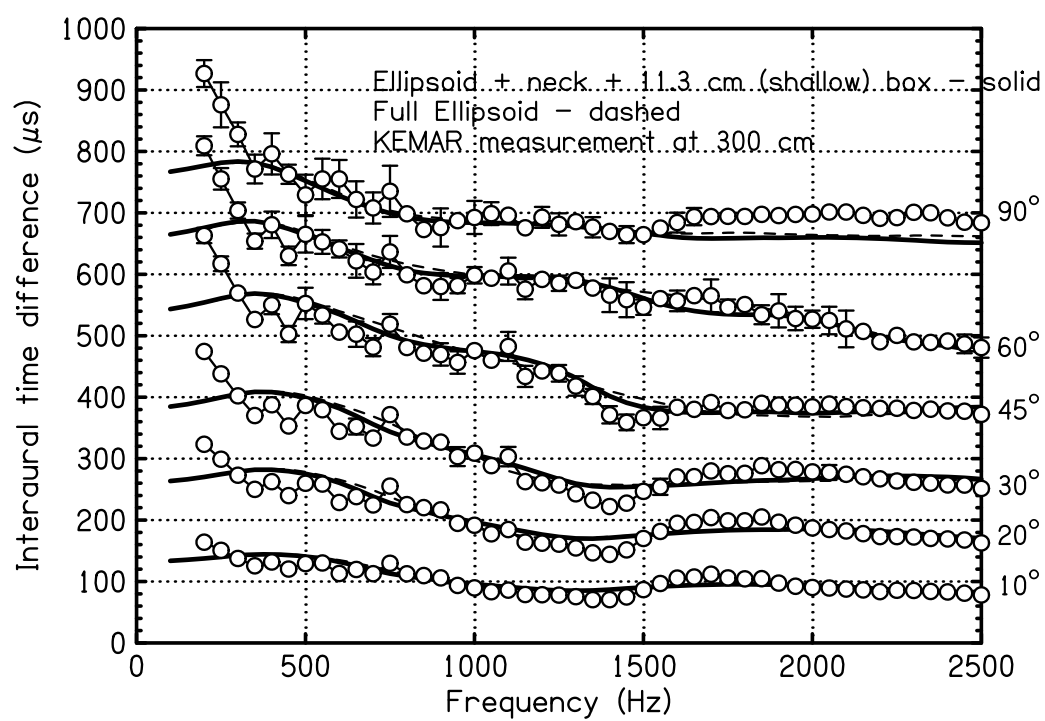


Fig. 2bx11itd

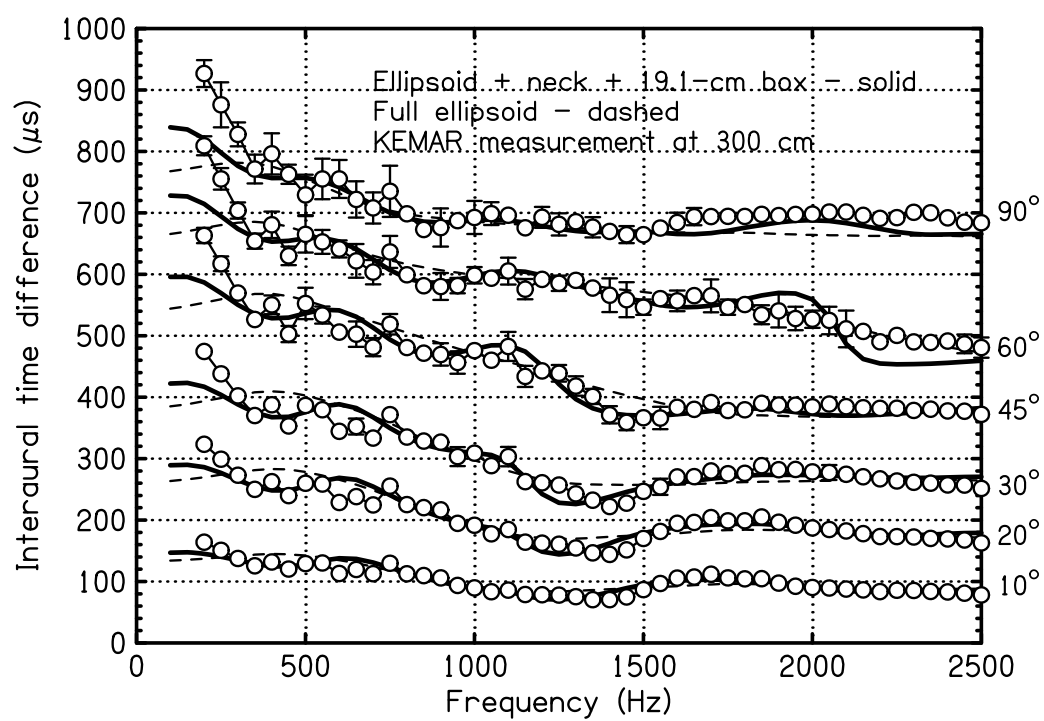


Fig. 2enbitd

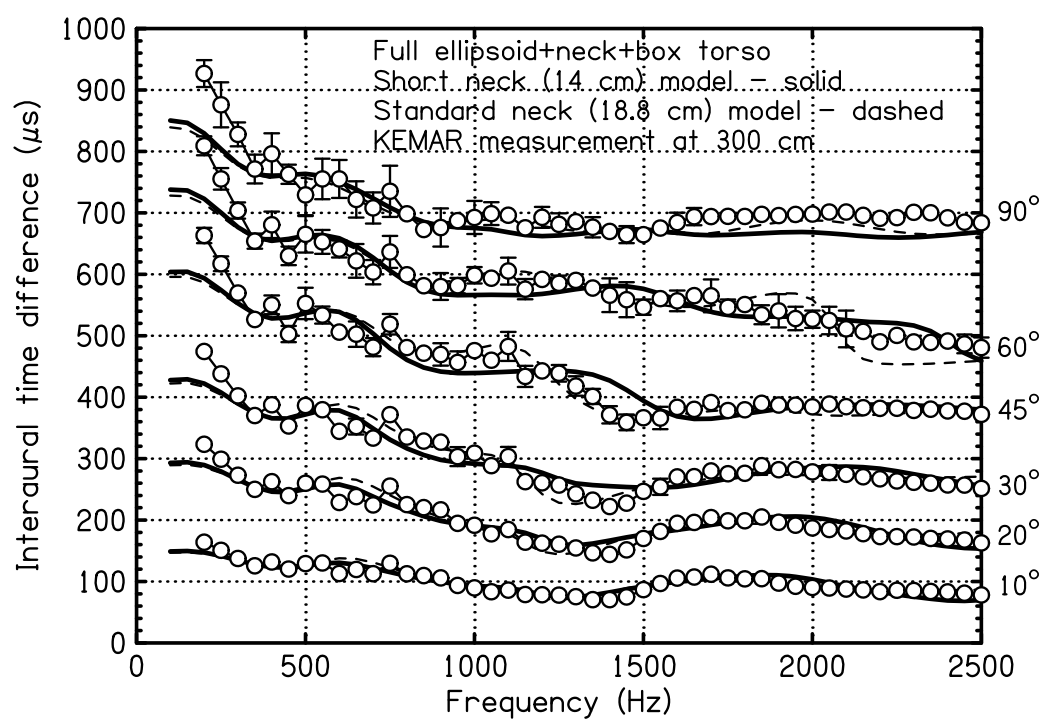


Fig. 2nk14itd

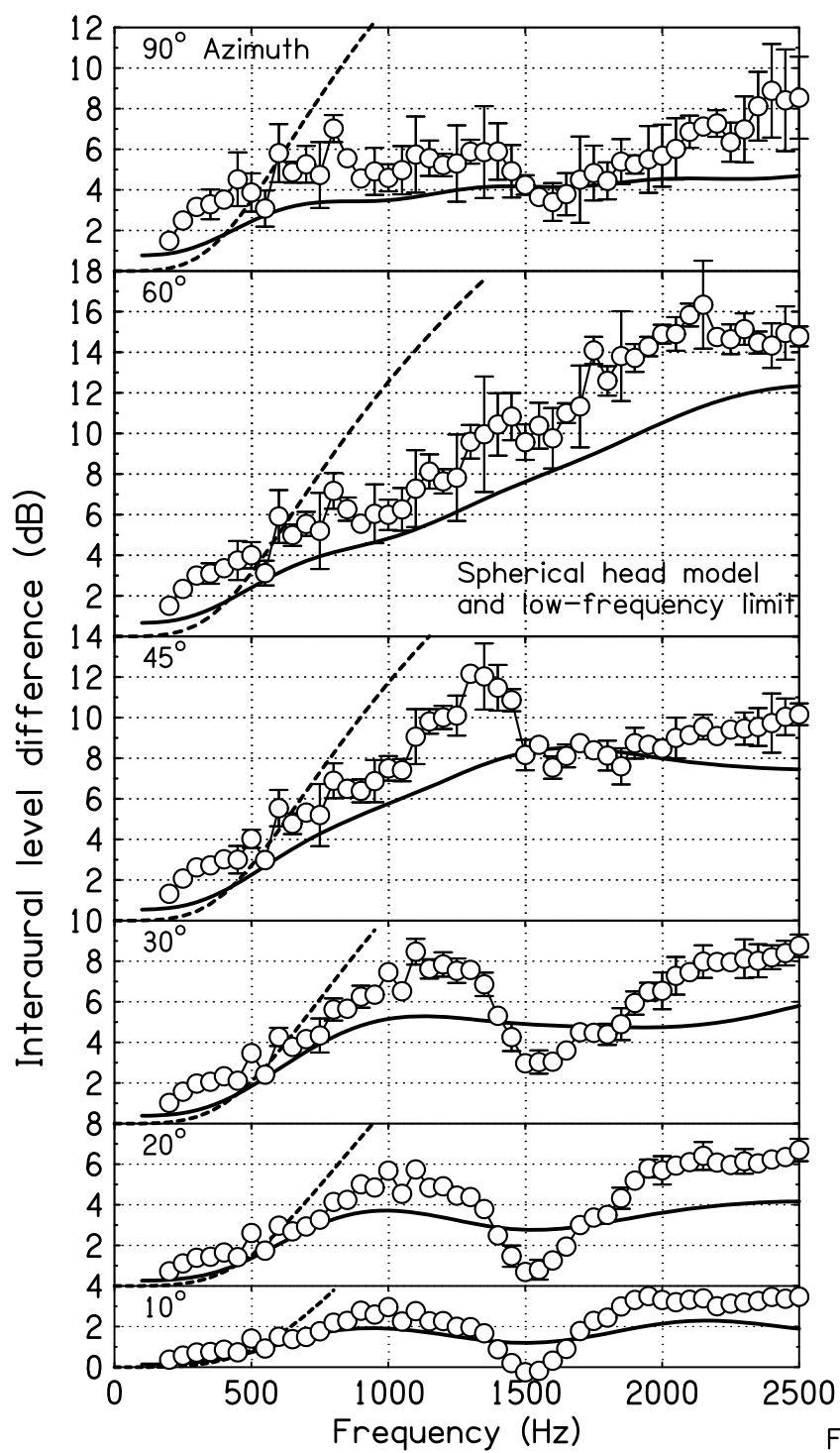


Fig. 2sh mild

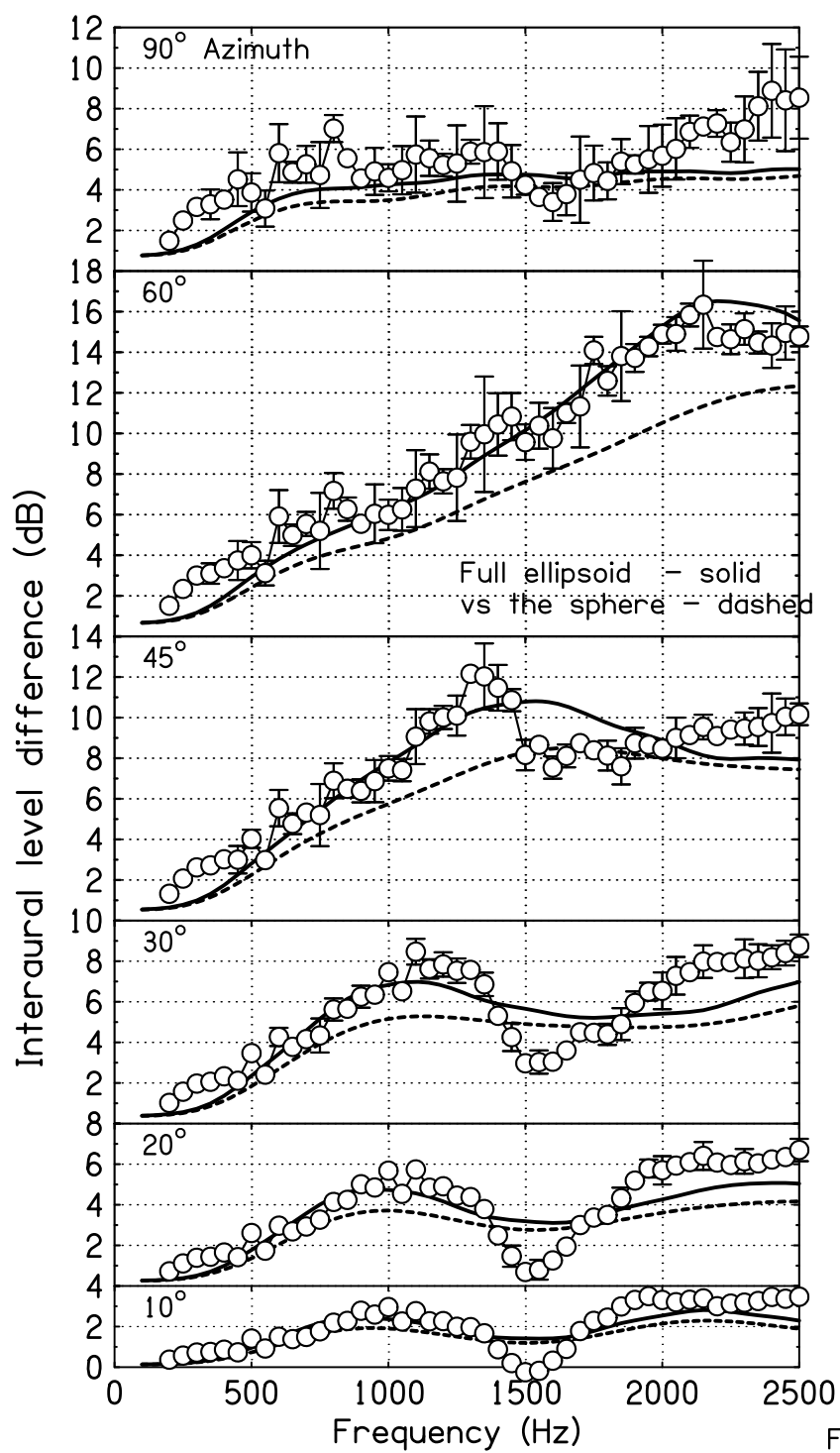


Fig. 2eild

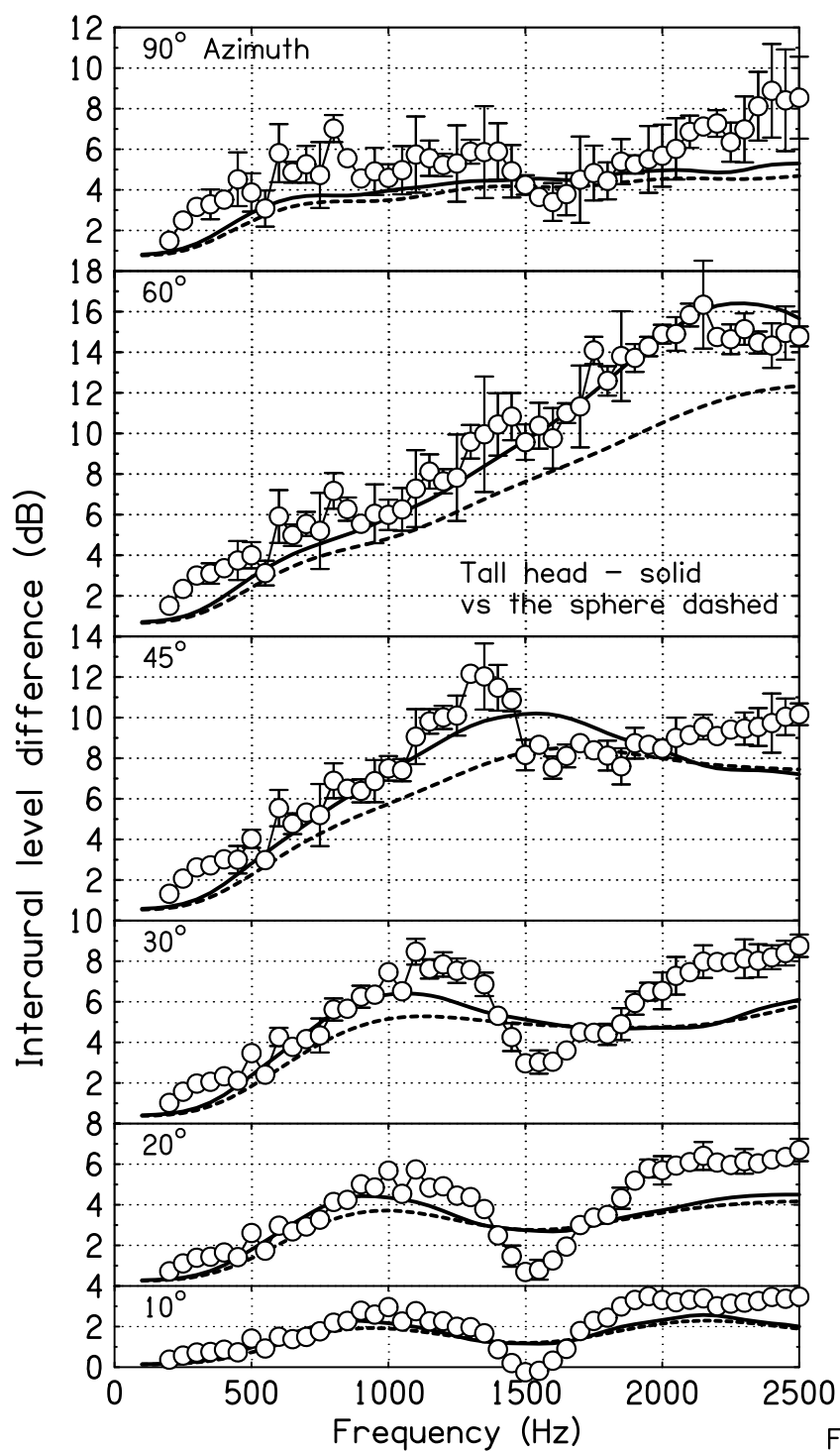


Fig. 2tallild

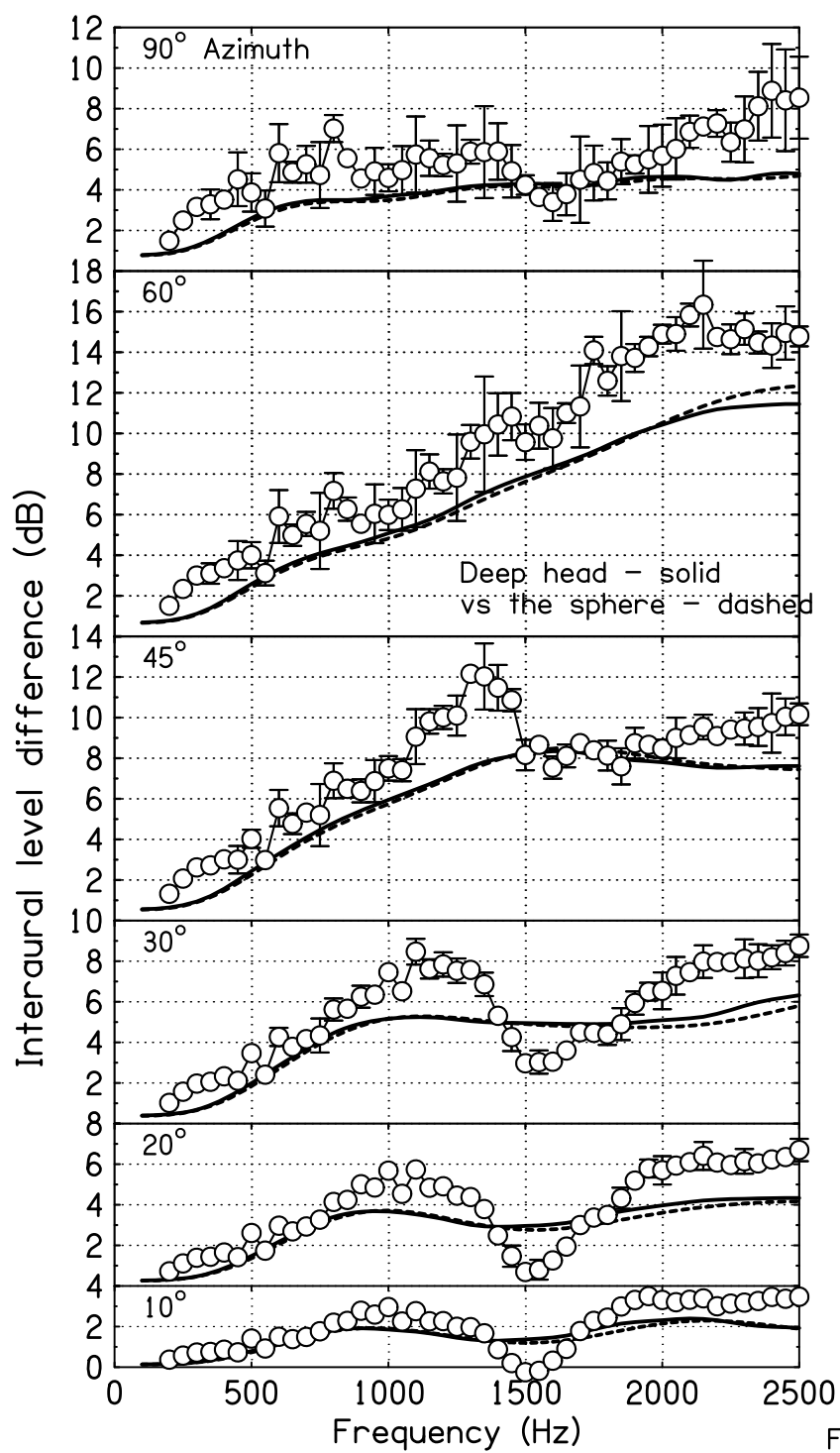


Fig. 2deepild

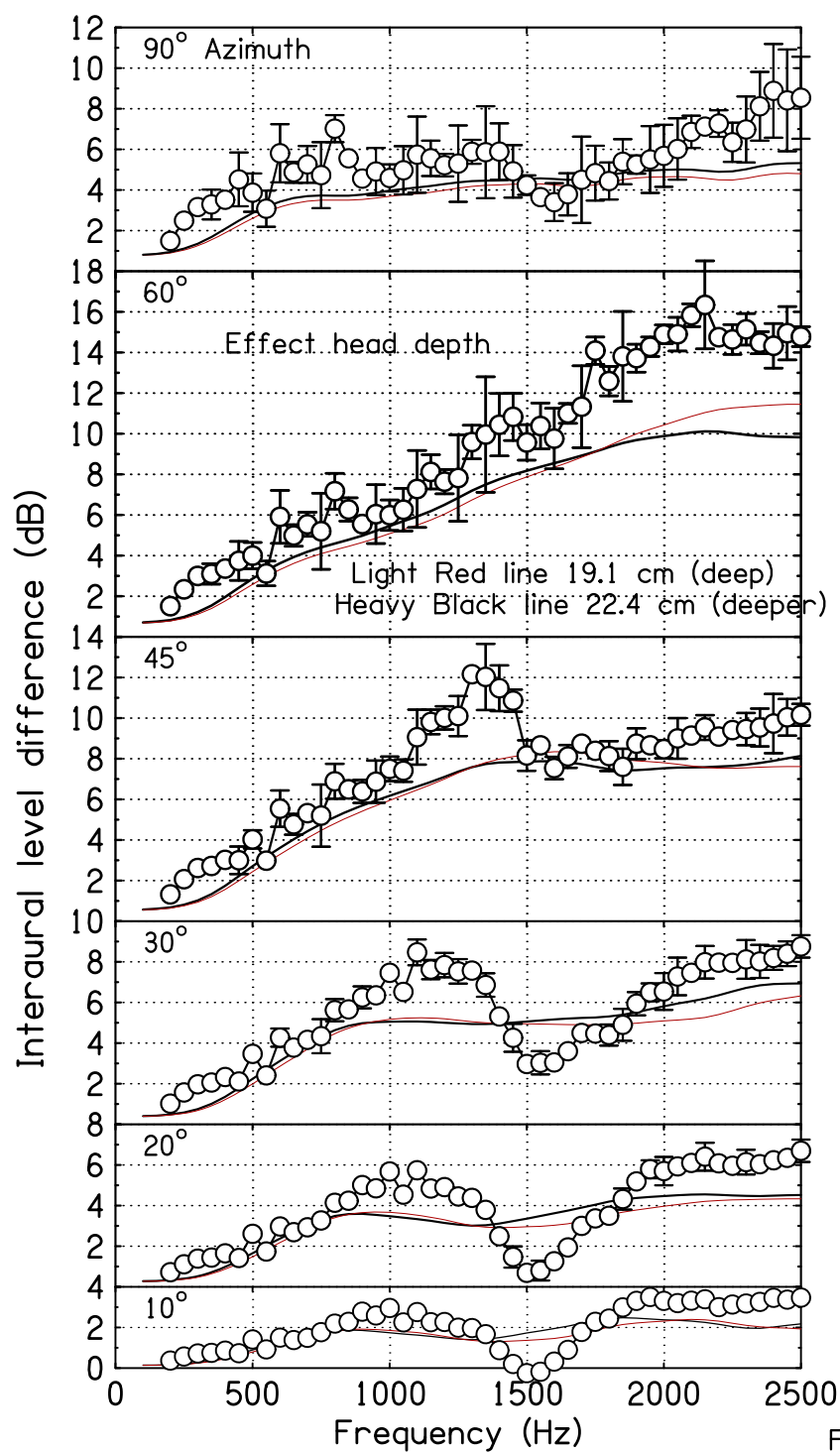


Fig. 2dperild

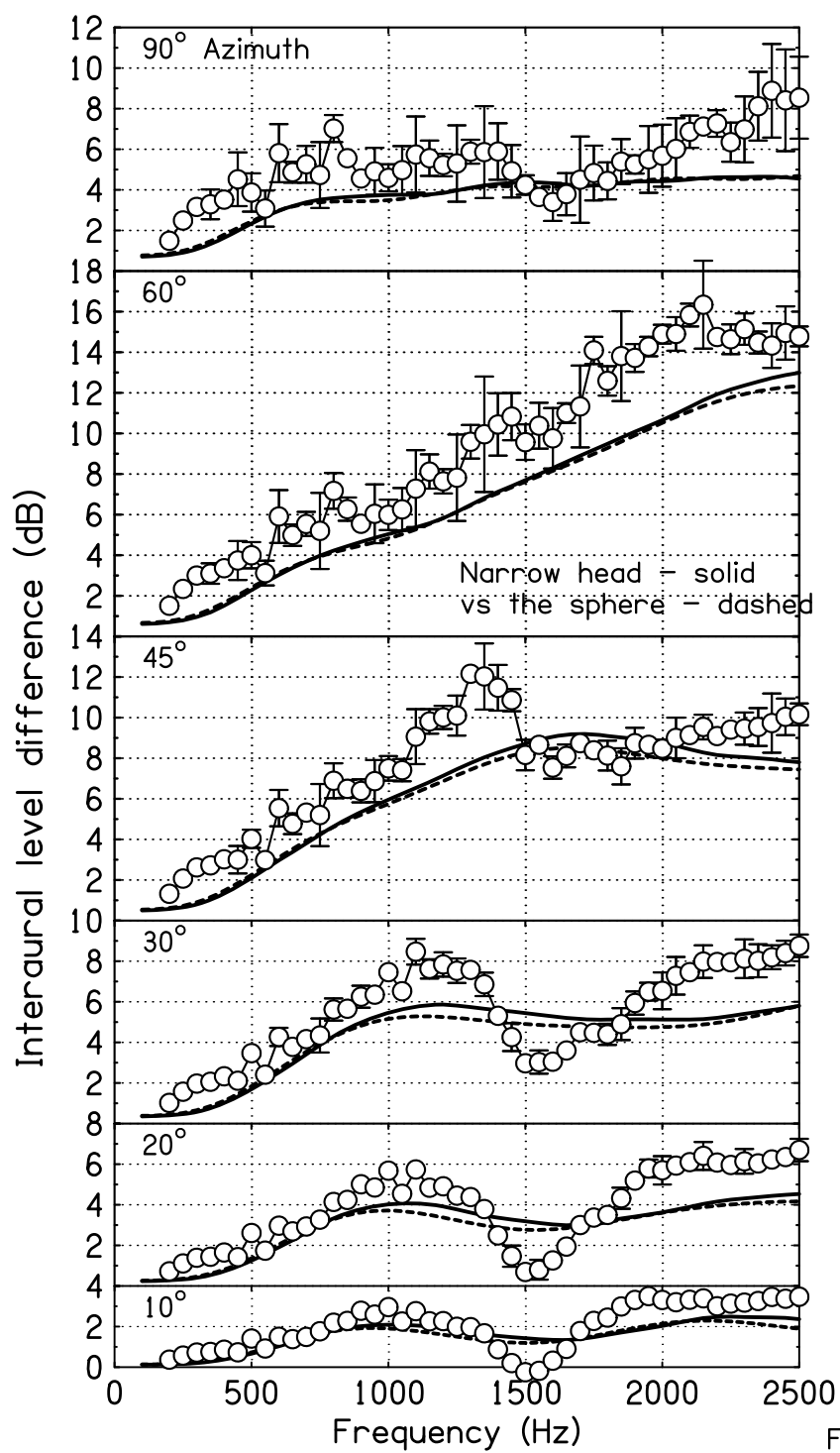


Fig. 2thinild

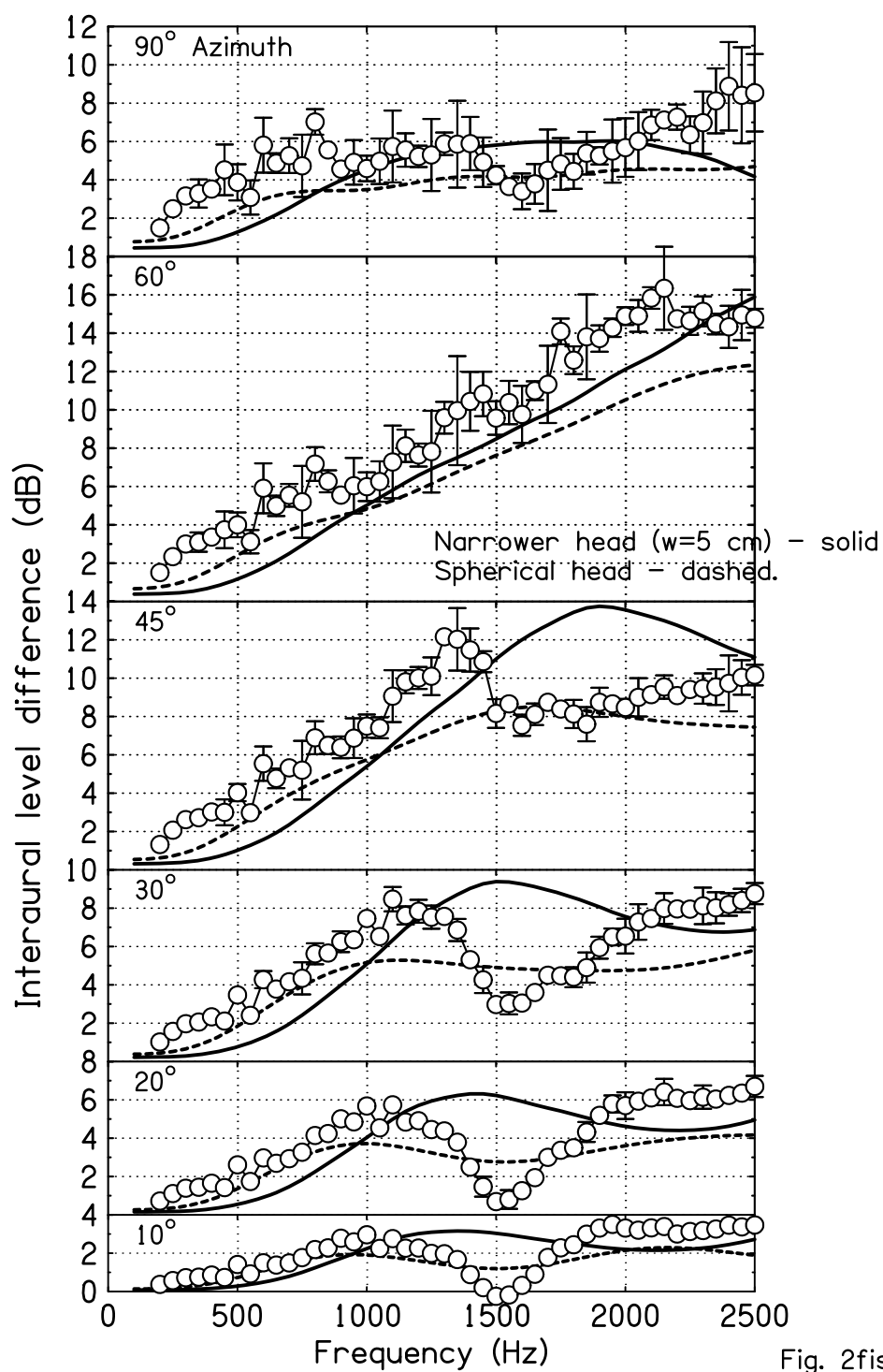


Fig. 2fishild

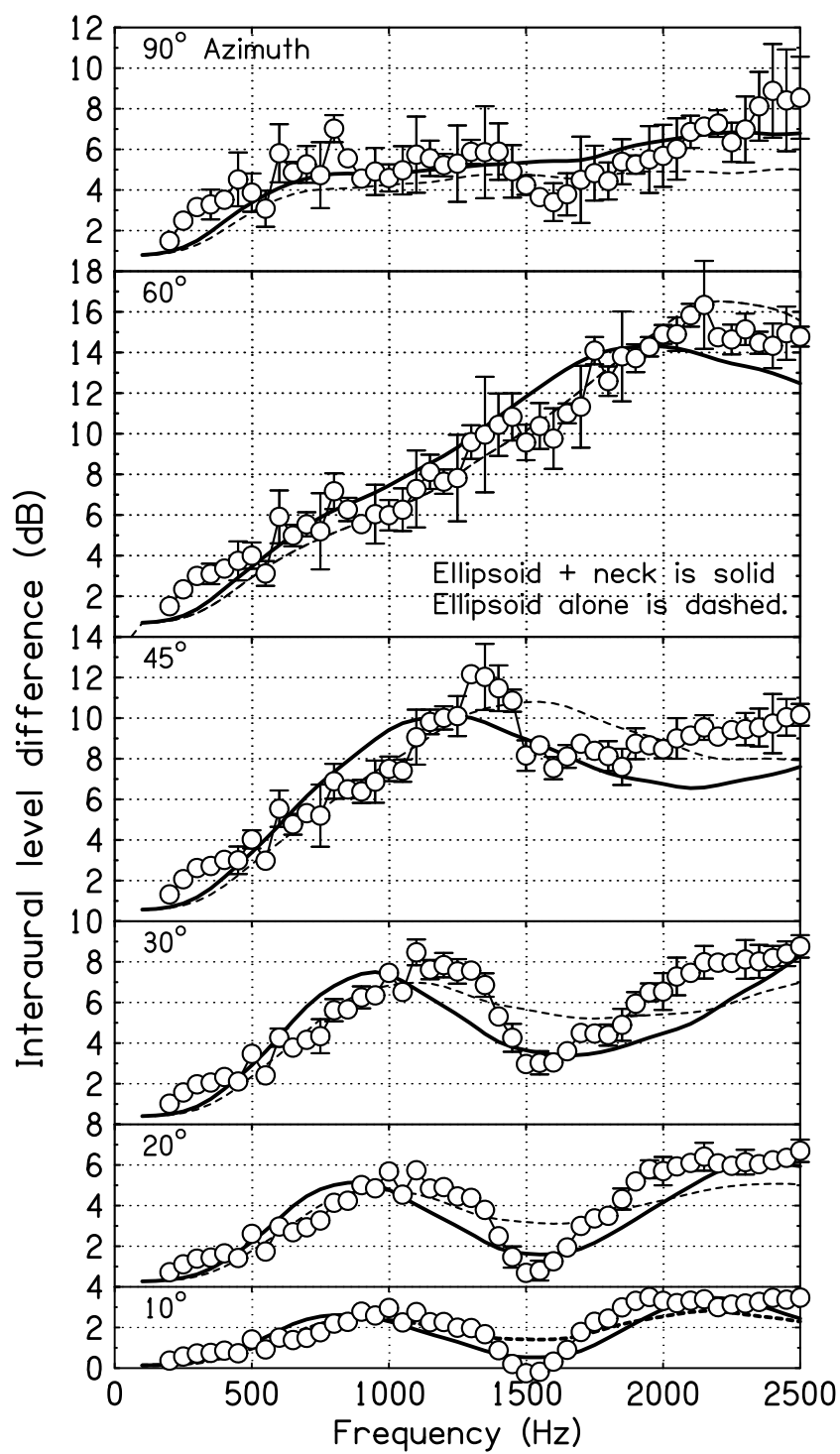


Fig. 2enild

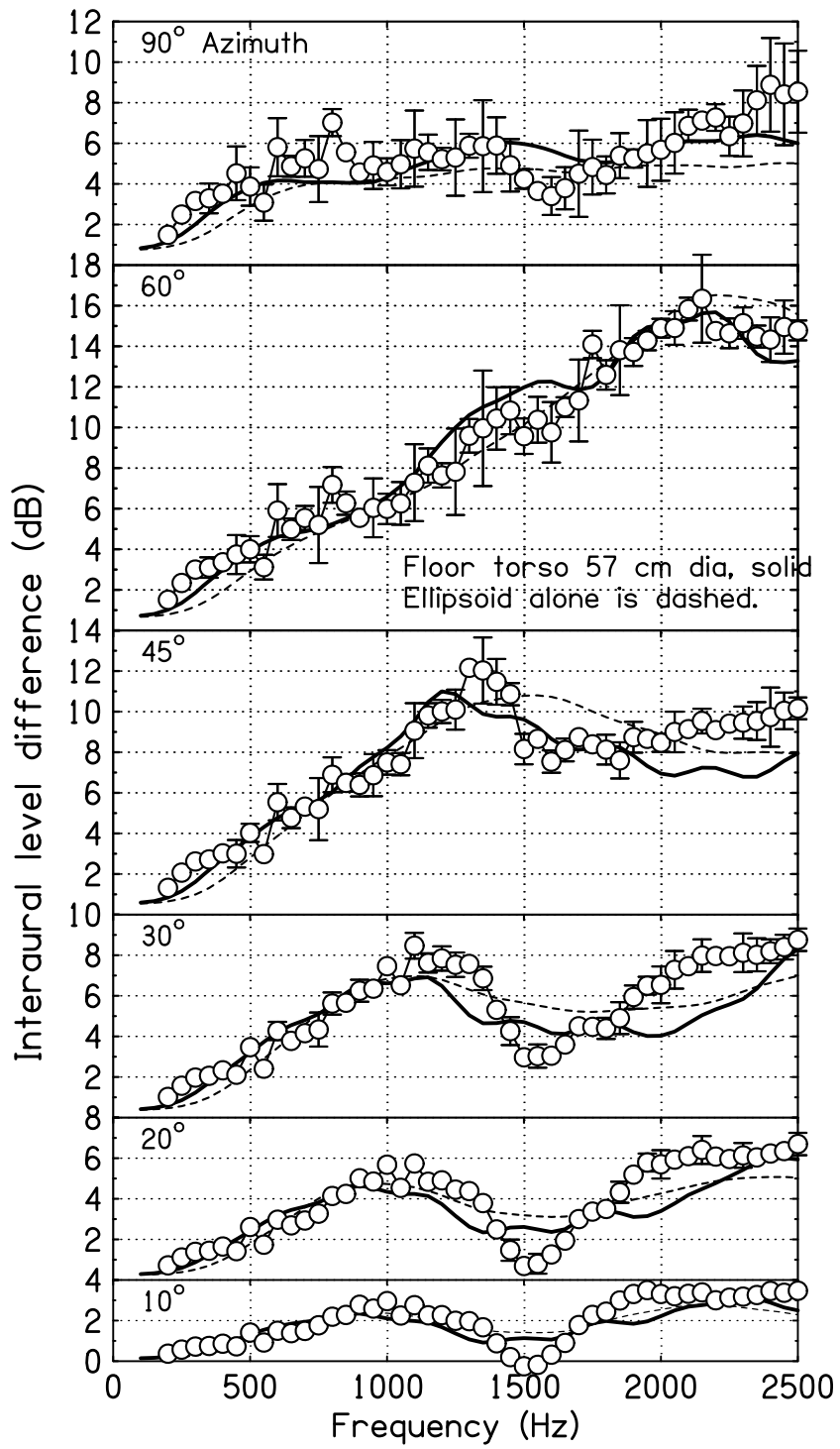


Fig. 2enfield

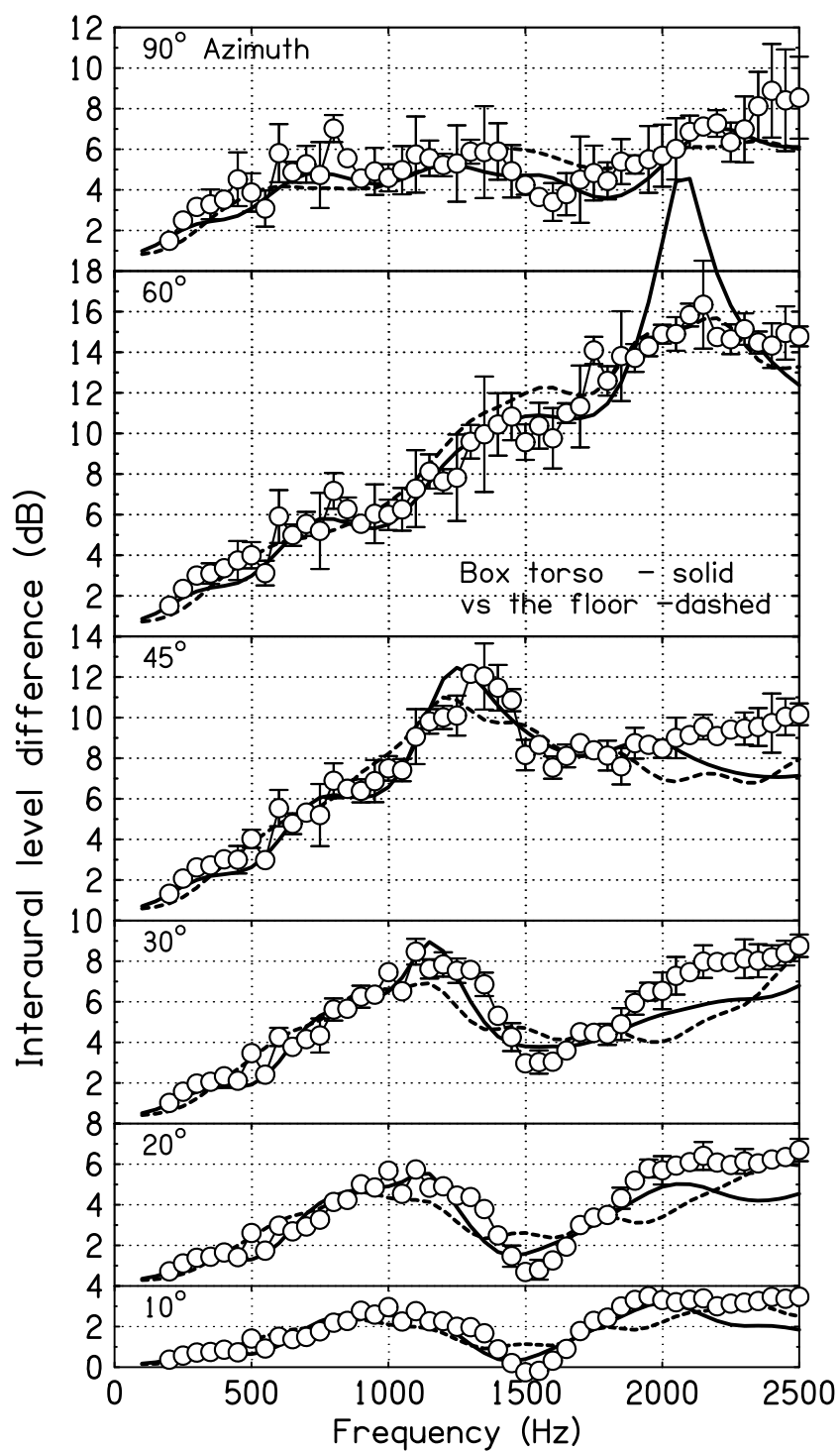


Fig. 2enbild

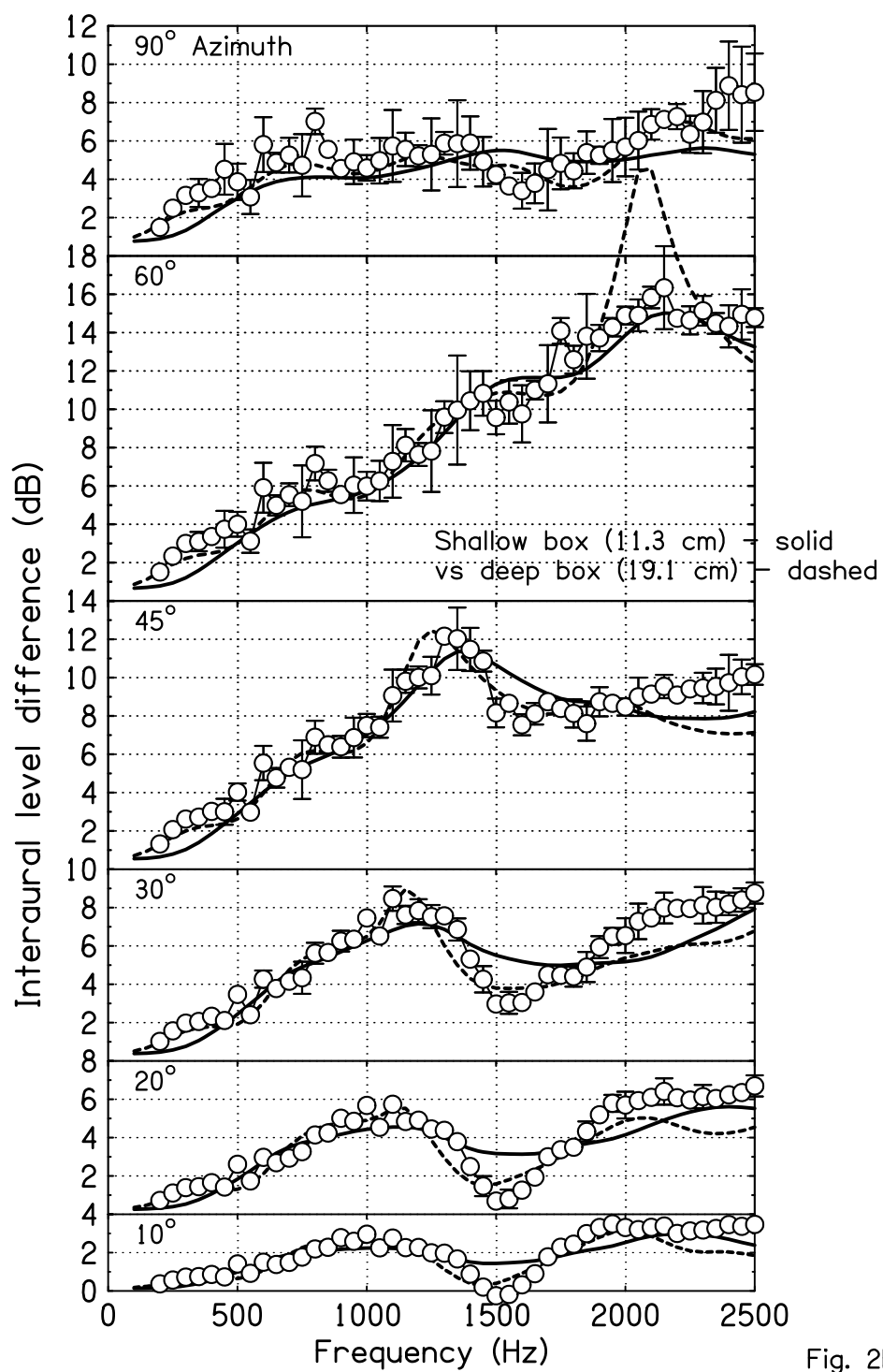


Fig. 2bx11ild

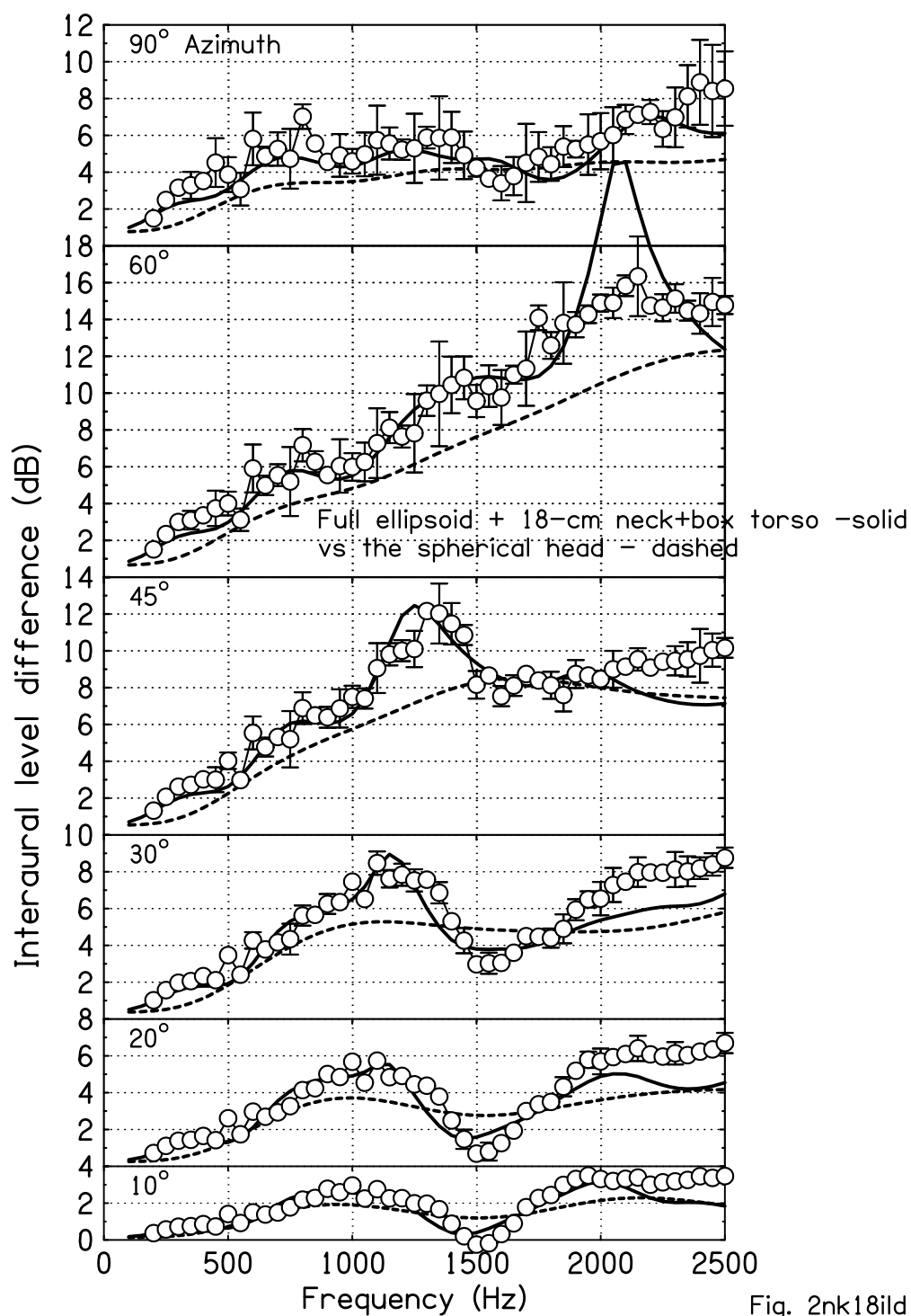


Fig. 2nk18ild

